International Journal of Engineering Research & Technology (IJERT)
ISSN: 2278-0181
Vol. 4 Issue 05, May-2015

Computational Analysis and Estimation of Drag Components through Mid Field Drag Decomposition Method

Shivakumar S. G.[1], Nagapp. L. P.[2], Shridevi S. K.[3]
[1,3]M.tech student, Department of Aeronautical Engineering, MVJCE, Bangalore
[2]Specialist (Air platform), IHS Global Pvt. Ltd., Bangalore
,

***Abstract*—Lift and drag are the most important parameters during cruise flight. A small increment in the drag costs more fuel. Therefore accurate prediction of aerodynamic drag is the key element. A computational method for drag decomposition is estimated. The mid field and near field methods are applied to NACA 0012 airfoil.The mid field drag decomposition method separates total drag into viscous, waveand spurious drag components. The spurious drag arises due to the numerical and truncation errors from the flow solution and hence elimination on the spurious drag inherently increases the accuracy of the flow solution. In this research, near field andmid field methods are applied to the airfoil for a transonicflow condition.**

Key words—Drag, Computational fluid dynamics,Near – Field Mid-Field method, spurious drag.

Nomenclature

a	=	speed of sound, m/s
ρ	=	density, kg/m^3
$\boldsymbol{V}$	=	velocity (u, v, w), m/s
U	=	unit tensor vector
n	=	unit normal vector (n_x, n_y, n_z)
S	=	surface area, m^2
p	=	pressure, N/m^2
s	=	entropy, J/K
D	=	drag, N
τ	=	shear stress tensor (τ_x, τ_y, τ_z), N/m^2
ΔH	=	Entropy, J/kg
Δs	=	change in entropy, J/K
γ	=	specific heat ratio
M	=	Mach number
R	=	gas constant
μ_l	=	Laminar viscosity, N s /m^2
μ_t	=	Turbulent viscosity,
Ω	=	Control volume, m^3

Subscripts

irrev	=	Irreversible
far	=	far field method
∞	=	freestream
vw	=	viscous and wave drag
v	=	viscous drag
w	=	wave drag
x, y, z	=	orthogonal coordinate system with x-axis points to the freestream.

I. INTRODUCTION

Aerodynamic drag is defined as the component of total force acting in the direction of relative wind. A small increment in the drag coefficient can lead to the significant increase in the operational cost of aircraft in the form of fuel price. That is increment of one drag count (=10^{-4} of total drag) adds a payload of 91kg to commercial transport aircraft [1]. There are basically two approaches as far as drag decomposition method is concerned. Firstly, the traditional approach to compute the drag from surface integration of pressure and skin friction around aircraft configuration and is commonly known as 'near-field method'. Second method is based on linear momentum principle known as 'far-field method' or 'wake integration method' [2]. That is it uses the wake integration on the Trefftz plane. This is indeed powerful aerodynamic tool because it breaks down the aerodynamic drag into its components. Last but not the least 'mid-field method' uses the flow field integration around the aircraft, this method is derived from the far-field formula given by Oswatitsch[3] who used Gauss divergence theorem to predict the drag.Classifications of these components are show in figure 1. In this research, the near field and mid field methods are applied to NACA 0012 airfoil configuration.

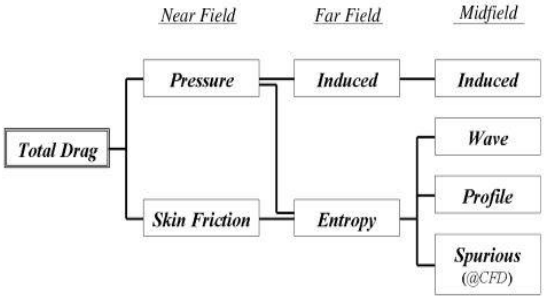

Fig. 1: Classification of drag components and methods.

Spurious drag mainly originates from the numerical dissipation and truncation errors; this drag is not related to the physical flow field. By eliminating the spurious drag created by entropy variations in the flow field, it is easy to predict the drag accurately for given aircraft configuration. There are some key things which are needed to be considered while separating the drag. The region where the shock wave interacts with viscous zone, these regions cannot be separated but with the help of shock sensor developed by Lovely and Hamis[4] and viscous sensor developed by Tognaccini[5], it is easy toseparate components of drag. These sensors identify which

cell belongs to shock region and which cell belongs to the viscous region. One major advantage of this method is accuracy of the solution is possible with the use of coarse grid.

II. ART OF DRAG DECOMPOSITION

A. Linear momentum theory

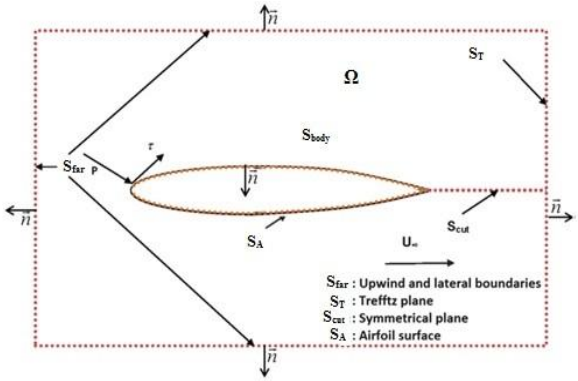

Fig. 2: control volume fixed in space.

Consider an aircraft in a steady state condition moving with velocity $\mathbf{V}_\infty$ as shown in figure 2. The aircraft is surrounded by a closed surface called control surface **S**, the volume inside the control surface is called control volume **Ω**. The aircraft is located far from the control surface **S** and applying the momentum theory to the closed control volume **Ω** yields [5]

$$\int_S [\rho \mathbf{VV} + p\mathbf{U} - \tau] \cdot \mathbf{n} dS = \int_S [\rho \mathbf{VV} + (p - p_\infty)\mathbf{U} - \tau] \cdot \mathbf{n} dS = 0 \quad (1)$$

The aircraft surface can be divided into S_{body} and S_{far} where S_{body} refers to the surface surrounding the aircraft and S_{far} is referring to the surface of far-field respectively. It is assumed that no slip taking place on the boundary walls i.e., V. n = 0 on S_{body}. Thus eqn. 1 can be written as

$$\mathbf{F} = \int_{S_{body}} [(p - p_\infty)\mathbf{n} - \tau \cdot \mathbf{n}] dS = - \int_{S_{far}} [\rho \mathbf{VV} + (p - p_\infty)\mathbf{U} - \tau] \cdot \mathbf{n} dS \quad (2)$$

Where,**F** is the total force acting on the body (for unpowered aircraft). This total force can be divided into two, computation of pressure and shear stress distribution on the body and estimation of the momentum balance on the outer boundaries of the domain.

Assuming the x-component of velocity, from eqn.2 far field drag can be written as

$$D_{far} = - \int_{S_{far}} [(p - p_\infty)n_x + \rho(u - u_\infty)(\mathbf{V} \cdot \mathbf{n}) - \tau_{xx} n_x - \tau_{xy} n_y - \tau_{xz} n_z] dS \quad (3)$$

Considering a force vector, **f**

$$\mathbf{f} = -\rho(u - u_\infty)\mathbf{V} - (p - p_\infty)\mathbf{n} + \tau_x \quad (4)$$

Therefore eqn. 3 can be written as

$$D_{far} = \int_{S_{far}} (\mathbf{f} \cdot \mathbf{n}) dS \quad (5)$$

From the eqn. 2 the far-field drag should be equal to the near field drag[6].

B. Thermodynamic variables

The far field method of integration permits the separation of total drag into its physical components such as viscous drag, wave drag and spurious drag which is an additional component arises because of the numerical and truncation errors. The breakdown of individual physical components of drag includes the difference between thermodynamic reversible and irreversible processes [7] due to the entropy variations in the flow field. Both the wave and viscous drags are irreversible processes which are related to the shock and boundary layer viscous effects whereas induced drag is an exchange of energy and hence it is reversible and is related to the vortices at the wing tip. To separate drag components it is necessary to introduce velocity defect, $\Delta\bar{u} = u - u_\infty$ which is mainly due to the irreversible process (eqn. 6) [8]

$$\frac{u}{u_\infty} = \sqrt{1 + 2\frac{\Delta H}{u_\infty^2} - \frac{2}{(\gamma - 1)M_\infty^2}\left[\left(\frac{\Delta p}{p_\infty} + 1\right)^{\frac{(\gamma-1)}{\gamma}} e^{\frac{\Delta S(\gamma-1)}{R\ \gamma}} - 1\right]} = f\left(\frac{\Delta p}{p_\infty}, \frac{\Delta S}{R}, \frac{\Delta H}{u_\infty^2}\right) \quad (6)$$

Eqn. 6 is valid for the airframe body. Expanding in Taylor's series we get,

$$\frac{u}{u_\infty} = 1 + f_{fp1}\frac{\Delta p}{p_\infty} + f_{fs1}\frac{\Delta S}{R} + f_{fH1}\frac{\Delta H}{u_\infty^2} + f_{fp2}\frac{\Delta p}{p_\infty} + f_{fs2}\frac{\Delta S}{R} + f_{fH2}\frac{\Delta H}{u_\infty^2} + f_{fps2}\frac{\Delta p}{p_\infty}\frac{\Delta S}{R} + f_{fpH2}\frac{\Delta p}{p_\infty}\frac{\Delta H}{u_\infty^2} + f_{fsH2}\frac{\Delta S}{R}\frac{\Delta H}{u_\infty^2} + O\left[\left(\frac{\Delta p}{p_\infty}\right)^3, \left(\frac{\Delta S}{R}\right)^3, \left(\frac{\Delta H}{u_\infty^2}\right)^3\right] \quad (7)$$

In the above equation the coefficients of expansion depend on γ and M_∞, and the first and second order terms can be written as

$$f_{fp1} = -\frac{1}{\gamma M_\infty^2}, \quad f_{fs1} = -\frac{1}{\gamma M_\infty^2}, \quad f_{fH1} = 1$$

$$f_{fp2} = -\frac{1 + \gamma M_\infty^2}{2\gamma^2 M_\infty^4}, \quad f_{fs2} = -\frac{1 + (\gamma - 1)M_\infty^2}{2\gamma^2 M_\infty^4}, \quad f_{fH2} = -\frac{1}{2}$$

$$f_{fps2} = -\frac{1 + (\gamma - 1)M_\infty^2}{\gamma^2 M_\infty^4}, \quad f_{fpH2} = \frac{1}{\gamma M_\infty^2}, \quad f_{fsH2} = \frac{1}{\gamma M_\infty^2}$$

From small perturbation approach, $\frac{\Delta S}{R} \ll 1$ and $\frac{\Delta H}{u_\infty^2} \ll 1$, the irreversible drag can be written as

$$D_{irrev} = - \int_{S_{far}} \rho \Delta u (\mathbf{V} \cdot \mathbf{n}) dS = \int_{S_{far}} \mathbf{f_{vw}} \cdot \mathbf{n} dS \quad (8)$$

Where, $\mathbf{f_{vw}}$ is force function with wave and viscous components and is given below

$$\mathbf{f_{vw}} = -\rho \Delta u \mathbf{V} \quad (9)$$

In the event of physical breakdown of drag through thermodynamic processes (effects of wave and viscous), initial step is to separate the axial velocity defect and in the eqn. 9Δu

indicates velocity defect in the stream wise direction which is due to the irreversible phenomena. In the upstream of the domain the velocity equals free stream velocity and pressure equals free stream pressure. Hence, the surface integral can be replaced by an integral over the downstream of the surface; this surface is located very far from the body [10]. The transformation of eqn. 8 i.e. surface to volume integral can be done with the help of Gauss theorem to get volume integration around the body. The eqn. 6 can be rewritten as

$$D_{irrev} = D_v + D_w = \int_{S_{far}} \mathbf{f_{vw}} \cdot \mathbf{n} dS = \int_{V} div\, \mathbf{f_{vw}} dV \quad (10)$$

Where, D_v and D_w are viscous and wave drag respectively, given below

$$D_v = \int_{V_V} div\ \mathbf{f_{vw}} dV \quad (11)$$

$$D_w = \int_{V_w} div\, \mathbf{f_{vw}} dV \quad (12)$$

The far-field drag formulation [6] ensures an exact nearfield/ far-field drag balance and is given below for two dimensional flow. In the case of three dimensions the induced drag term will added to the right side of the eqn. 13 [11].

$$C_{D_p} + C_{D_f} = C_{D_v} + C_{D_w} + C_{D_{sp}} \quad (13)$$

C. Wave and viscous sensors

To detect shock region, a sensor based algorithm developed by Lovely and Haimes[4] function is introduced.

$$f_{shock} = \frac{\mathbf{V} \cdot \nabla p}{a|\nabla p|} \quad (14)$$

This sensor activates whenever it satisfies the followingcondition $f_{shock} \geq 1$.

To detect the region influenced by viscosity, a sensor based algorithm developed by Tognaccini [5] is implemented into the code.

$$f_{viscous} = 1 + \frac{\mu_t}{\mu_l} \quad (15)$$

The viscous region is identified whenever its value is greater than 1.1 times the free-stream value of the same.

III. Numerical Modeling

The CFD study is carried out on a transonic NACA 0012 airfoil, the domain is of C-type topology. This geometry is shown in fig. 3.

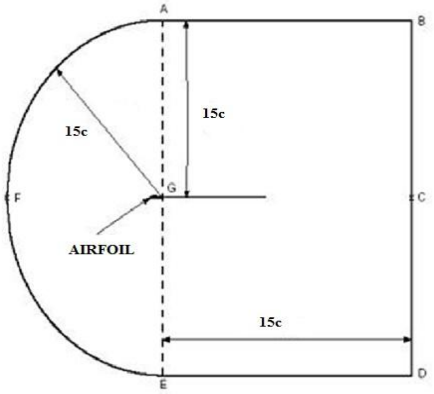

Fig. 3: Geometry specifications.

In this research, a finer grid is used; this consists of structured grid with C-type topology. Useful information about the airfoil is found in NASA Validation center. The fine grid has0.33 million cells for Mach number 0.799 at an angle of attack 2.26^0 with Reynolds number $9.0 * 10^6$ and the y^+ value is taken as 0.5 for fine. The shock and viscous regions are detected by their respective sensor algorithms which require finer grid as well as low y^+ values to capture the required flow regions accurately [9].

IV. Results and Discussions

A. Validation

The simulationsare carried out using ANSYS-Fluent 15.0. The implicit method is used with Green Gauss Node based recursion gradient method and the second order upwind scheme is considered. For all the test cases, the *k*-ω shear stress transport (SST) turbulence model is used. For each computation, the converged residuals were in the range of 10^{-5} to 10^{-7}, usually achieved within 8000 iterations. Each run is started from free-stream conditions. The iterative convergence is studied and thevalidation of the NACA0012 airfoil has been conducted. The comparisons of computational and experimental results are shown in fig. 4.

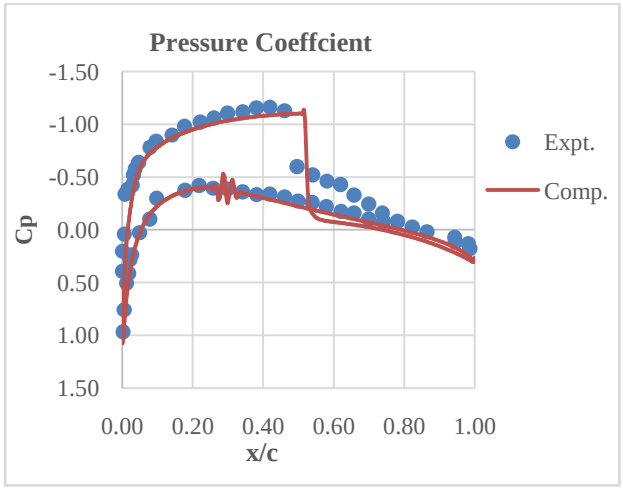

Fig. 4: Validation of surface pressure distribution for $M_\infty = 0.799\ at\ \alpha = 2.26^0$.

	Computational	Experimental
C_D	0.033755	0.0331
C_L	0.390	0.4438545
C_m	-0.0203	-0.0196891

Table 1: Comparison of lift, drag and moment coefficients.

B. 2D drag decomposition

The estimation of near field and mid field drag have been carried out as follows. An algorithm is developed using the C language to read the solution of the above and to compute the integrals of drag components (from eqn. 11 and 12) including the spurious drag. Latter the spurious drag is eliminated from the equation 13 which equals the near field and far field drag.

Drag Decomposition		
Components	Mid field Method	Near field Method
$C_{D_{Viscous}}$	298.7032	337.55
$C_{D_{Wave}}$	21.974	
$C_{D_{Spurious}}$	10.165	
$C_{D_{Total}}$	330.8422	

Table. 2: NACA 0012 viscous test, $M_\infty = 0.799\ at\ \alpha = 2.26^0$

All the values are given in the drag counts (1 count =10^{-4}). The drag breakdown for NACA 0012 airfoil is given in the table 2. Mid field drag consists of viscous, wave and spurious drag. From the drag breakdown analysis it is observed that the spurious drag is estimated is about 10.165 counts. This means the spurious drag can be taken into consideration in the aerodynamic design. From the analysis of drag decomposition method, by eliminating the spurious drag contribution it is possible to estimate accurate drag components' values.

This analysis provides the visualization of the each drag components. The shock, viscous and spurious zones are visualized and are shown in fig. 6, 7 and 8 respectively.

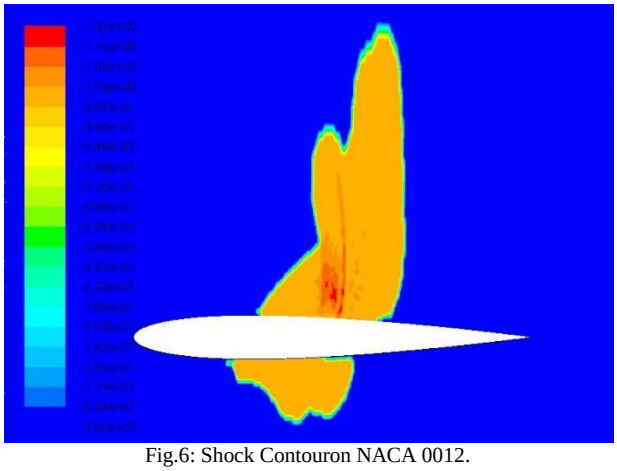

Fig.6: Shock Contouron NACA 0012.

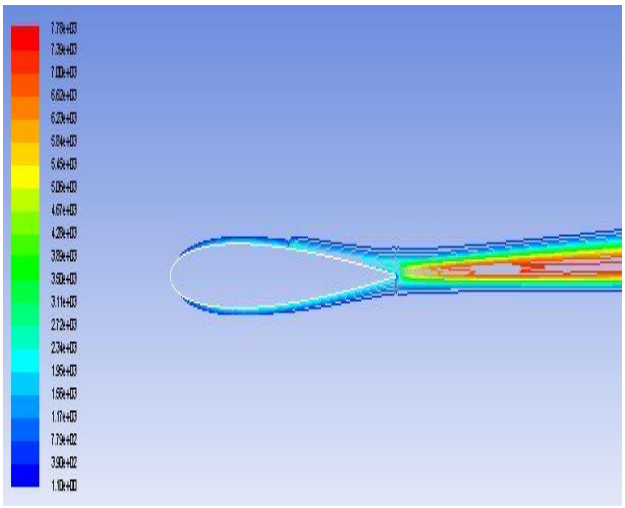

Fig. 7: Viscous region observed on the NACA 0012.

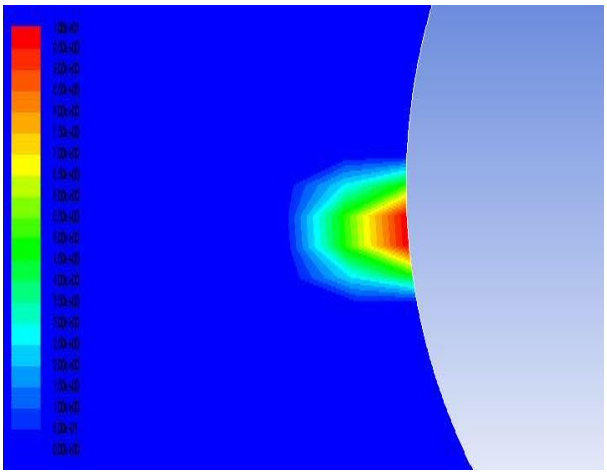

Fig. 8: Spurious Contribution observed on the leading edge of the airfoil.

V. CONCLUSIONS

The computational method is used to calculate the flow field around a NACA 0012airfoil.The iterative convergence criteriais studied and tested, it is found that residual target up to the value of 10^{-7} has been achieved. The computational results are validated with the experimental results for Mach number 0.799, Reynolds number 9.0 * 10^6 and angle of attack 2.26^0. From the post processing results, the visualization of the shock, viscous and spurious zones are observed. An algorithm is developed using C language to compute each drag components.The physical breakdown of total drag into viscous, wave and spurious drag components has been estimated. It is important to note that the spurious drag mainly arises due to the large flow field gradients occurs at the leading edges of the wing, nacelle and nose of the fuselage. This spurious drag contribution is observed clearly at the leading edge of the airfoil and the amount of this contribution is also estimated. Thus, by eliminating spurious drag contribution it is possible to predict accurate drag coefficient.

ACKNOWLEDGEMENTS

This research is conducted at MVJ College of Engineering, Bangalore, India. I express my sincere gratitude to Nagapp. L.P. for providing excellent guidance throughout the research. The high class facility at MVJCEhas allowed to complete the task. I also thank my co-author Shridevi S.K. for continued encouragement and support.

REFERENCES

[1] Meredith, P., "Viscous Phenomena Affecting High Lift Systems And Suggestions For Future CFD Development", AGARD TR-94 18415-04-01, Sept. 1993.

[2] Kazuhiro Kusunose, "Drag prediction based on a wake integral method", AIAA- 98-2723

[3] Oswatitsch, K., Gas Dynamics, Academic Press, New York, 1956, pp. 177–210

[4] Lovely, D., and Haimes, R., "Shock Detection from Computational Fluid Dynamics Results," AIAA Paper 1999-3285, 1999.

[5] Tognaccini T., Methods for Drag Decomposition, Thrust-Drag Bookkeeping from CFD Calculations, VKI Lecture SeriesCFD-Based Aircraft Drag Prediction and Reduction, VKI LS 2003-02, 2003

[6] D.Destarac, “Far Field Drag Extraction from the Hybrid Computations”, AIAA DPW-2, Orlando, 21-22 June 2003
[7] Martin Gariépy,Benoit Malouin, Jean-Yves Trépanier, and Éric Laurendeau, “Far-Field Drag Decomposition Applied to the Drag PredictionWorkshop 5 Cases”, Journal of Aircraft, DOI: 10.2514/1.C032204
[8] Jan B. Vos, Stephane Sanchi, and Alain Gehri, “DPW4 Results Using Different Grids IncludingNear-Field/Far-Field Drag Analysis”, AIAA, pp. 1-20.
[9] Salim M. and S.C. Cheah, “Wall y^+ Strategy for Dealing with Wall-bounded Turbulent Flows”, Proceedings of the International MultiConference of Engineers and Computer Scientists 2009 Vol IIIMECS 2009, March 18 - 20, 2009, Hong Kong, ISBN: 978-988-17012-7-5
[10] Wataru Yamazaki,Kisa Matsushima and Kazuhiro Nakahashi, “Aerodynamic Design Optimization Usingthe Drag-Decomposition Method”, AIAA Journal Vol. 46, No. 5, May 2008, DOI: 10.2514/1.30342.
[11] D. Destarac and J. van der Vooren, “Drag/thrust analysis of jet-propelled transonic transport aircraft;Definition of physical drag components”, Aerospace Science and Technology 8 (2004) 545–556